
This is an electronic reprint of the original article.

This reprint may differ from the original in pagination and typographic detail.

Milardovich, Diego; Souza, Victor H.; Zubarev, Ivan; Tugin, Sergei; Nieminen, Jaakko O.; Bigoni, Claudia; Hummel, Friedhelm C.; Korhonen, Juuso T.; Aydogan, Dogu B.; Lioumis, Pantelis; Taherinejad, Nima; Grasser, Tibor; Ilmoniemi, Risto J.

DELMEP : a deep learning algorithm for automated annotation of motor evoked potential latencies

Published in:
Scientific Reports

DOI:
[10.1038/s41598-023-34801-9](https://doi.org/10.1038/s41598-023-34801-9)

Published: 01/12/2023

Document Version
Publisher's PDF, also known as Version of record

Published under the following license:
CC BY

Please cite the original version:
Milardovich, D., Souza, V. H., Zubarev, I., Tugin, S., Nieminen, J. O., Bigoni, C., Hummel, F. C., Korhonen, J. T., Aydogan, D. B., Lioumis, P., Taherinejad, N., Grasser, T., & Ilmoniemi, R. J. (2023). DELMEP : a deep learning algorithm for automated annotation of motor evoked potential latencies. *Scientific Reports*, 13(1), 1-11. Article 8225. <https://doi.org/10.1038/s41598-023-34801-9>



OPEN

DELMEP: a deep learning algorithm for automated annotation of motor evoked potential latencies

Diego Milardovich^{1,2,3,13}✉, Victor H. Souza^{1b,2,3,4,13}, Ivan Zubarev^{1b,2}, Sergei Tugin^{1b,2,3,5,6}, Jaakko O. Nieminen^{1b,2,3}, Claudia Bigoni^{1b,7,8}, Friedhelm C. Hummel^{1b,7,8,9}, Juuso T. Korhonen^{1b,2}, Dogu B. Aydogan^{1b,2,10}, Pantelis Lioumis^{1b,2,3}, Nima Taherinejad^{1b,11,12}, Tibor Grasser^{1b,1} & Risto J. Ilmoniemi^{1b,2,3}

The analysis of motor evoked potentials (MEPs) generated by transcranial magnetic stimulation (TMS) is crucial in research and clinical medical practice. MEPs are characterized by their latency and the treatment of a single patient may require the characterization of thousands of MEPs. Given the difficulty of developing reliable and accurate algorithms, currently the assessment of MEPs is performed with visual inspection and manual annotation by a medical expert; making it a time-consuming, inaccurate, and error-prone process. In this study, we developed DELMEP, a deep learning-based algorithm to automate the estimation of MEP latency. Our algorithm resulted in a mean absolute error of about 0.5 ms and an accuracy that was practically independent of the MEP amplitude. The low computational cost of the DELMEP algorithm allows employing it in on-the-fly characterization of MEPs for brain-state-dependent and closed-loop brain stimulation protocols. Moreover, its learning ability makes it a particularly promising option for artificial-intelligence-based personalized clinical applications.

The motor evoked potential (MEP) generated by transcranial magnetic stimulation (TMS) is a crucial neurophysiological signal in research and clinical practice. MEP amplitude and latency allow us to assess quantitatively the corticospinal excitability. This is necessary to evaluate patients undergoing surgery and to monitor neuro-motor diseases, such as the progression of multiple sclerosis¹, the recovery of stroke patients² and idiopathic generalized epilepsy patients³, among a wide range of medical applications. MEPs are commonly characterized by their latency, which is defined as the time elapsed between the stimulation and the onset of the MEP (Fig. 1). The MEP latency is usually annotated manually after visual inspection of the electromyography (EMG) recording, making the process time-consuming, operator-dependent, and prone to errors^{4,5}. An algorithm to automate the characterization of MEPs would not only save time and reduce human errors, but would also boost the development of brain-state-dependent and closed-loop brain stimulation protocols by allowing accurate real-time MEP assessment⁶.

Several attempts have been made to develop algorithms to automate the MEP latency annotation. These algorithms are based either on absolute hard threshold estimation (AHTE)⁷ or on statistical measures^{8,9}. A review and comparison of previous methods is presented by Šoda et al.¹⁰, together with their own algorithm named Squared

¹Institute for Microelectronics, Technische Universität Wien, Gußhausstraße 27-29/E360, 1040 Vienna, Austria. ²Department of Neuroscience and Biomedical Engineering, Aalto University School of Science, Espoo, Finland. ³BioMag Laboratory, HUS Medical Imaging Center, University of Helsinki, Aalto University and Helsinki University Hospital, Helsinki, Finland. ⁴School of Physiotherapy, Federal University of Juiz de Fora, Juiz de Fora, MG, Brazil. ⁵Department of Neurology, Stanford University School of Medicine, Stanford, CA, USA. ⁶Department of Psychiatry and Behavioral Sciences, Stanford University School of Medicine, Stanford, CA, USA. ⁷Defitech Chair of Clinical Neuroengineering, Neuro-X Institute (INX) and Brain Mind Institute (BMI), École Polytechnique Fédérale de Lausanne (EPFL), 1202 Geneva, Switzerland. ⁸Defitech Chair of Clinical Neuroengineering, Neuro-X Institute (INX) and Brain Mind Institute (BMI), École Polytechnique Fédérale de Lausanne (EPFL Valais), Clinique Romande de Réadaptation, 1951 Sion, Switzerland. ⁹Clinical Neuroscience, Geneva University Hospital (HUG), 1205 Geneva, Switzerland. ¹⁰A. I. Virtanen Institute for Molecular Sciences, University of Eastern Finland, Kuopio, Finland. ¹¹Institute for Computer Technology, Technische Universität Wien, Vienna, Austria. ¹²Institute of Computer Engineering, Heidelberg University, Heidelberg, Germany. ¹³These authors contributed equally: Diego Milardovich and Victor H. Souza. ✉email: milardovich@iue.tuwien.ac.at

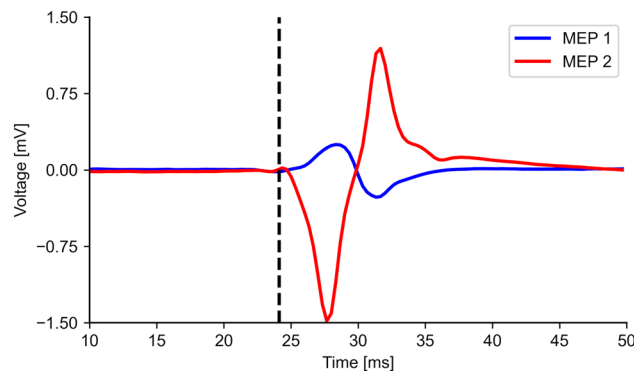


Figure 1. Two different MEP waveforms (red and blue curves) with similar latencies (black vertical line), defined as the time elapsed between the TMS and the beginning of the MEP trace. The epoch starts at the time the TMS pulse is delivered.

Hard Threshold Estimator (SHTE). In general, the previously presented algorithms require the user to specify a set of so-called *magic numbers*. These are hyperparameters with a large impact on the algorithm performance, which are empirically derived and depend on the user's knowledge and experience¹⁰. On the other hand, Bigoni's method¹¹, which is a derivative-based algorithm, does not require the user to specify magic numbers.

Developing an algorithm to automate the annotation of MEPs is not trivial. Even in ideal conditions of high signal-to-noise ratio (SNR), MEPs are highly variable, presenting significant inter- and within-subject amplitude variability^{12–14}. Similarly, the MEP latency variability is well known and has been previously documented for neurosurgical patients^{12,15}. Under similar circumstances, the amplitude of two MEPs can differ up to an order of magnitude and present totally different shapes, as shown in Fig. 1. Furthermore, low-amplitude MEPs, commonly recorded in inhibitory stimulation paradigms with paired-pulse TMS have inherently lower SNR than high-amplitude MEPs, thus adding a new layer of complexity. Overall, these factors make it demanding to assess the MEP latency automatically and reliably.

In this context, machine-learning-based algorithms, particularly those employing deep learning techniques, offer a promising approach to provide an accurate and reliable solution. The MEP latency annotation is a pattern recognition problem, where deep learning methods have already demonstrated their potential¹⁶. In this work, we present our DELMEP algorithm, which relies on deep learning for automated MEP latency annotation. We contend that DELMEP will speed up data analysis procedures and facilitate the development of closed-loop brain stimulation protocols, as well as the development of personalized medical solutions. To the best of our knowledge, this is the first deep learning solution to the problem of automating the MEP latency estimation.

Material and methods

MEP dataset. We utilized a dataset collected from 9 healthy volunteers (3 women and 6 men, mean age: 30 years, range 24–41) for two studies^{17,18}, which describe the detailed experimental protocol and stimulation paradigms. Experiments were performed in accordance with the Declaration of Helsinki and approved by the Coordinating Ethics Committee of the Hospital District of Helsinki and Uusimaa. All participants gave written informed consent before their participation.

TMS was applied with a monophasic trapezoidal waveform by our custom-made multi-channel TMS (mTMS) power electronics¹⁹ connected to a 2-coil transducer capable of electronically rotating the peak induced electric field¹⁷. EMG signals were digitized using an eXimia EMG 3.2 system (Nexstim Plc, Finland; sampling frequency 3 kHz; 10–500 Hz band-pass filter). MEPs were collected with single-pulse and paired-pulse paradigms. The paired-pulse stimuli were delivered with interstimulus intervals of 0.5 and 1.5 ms (short-interval intracortical inhibition, low-amplitude MEPs) and 6.0 and 8.0 ms (intracortical facilitation, high-amplitude MEPs). The conditioning stimulus intensity was 80% of resting motor threshold and the test stimulus and single pulse intensity were both 110% of resting motor threshold. MEPs were recorded from the abductor pollicis brevis, abductor digiti minimi and first dorsal interosseous muscles. EMG recordings showing muscle pre-activation or movement artifacts greater than $\pm 15 \mu\text{V}$ within 1 s before the TMS pulse were removed from the analysis. The raw MEPs were visually inspected, and the latency was manually annotated by a single expert (doctoral candidate; 7 years of experience) and quality-checked by a second expert (postdoctoral researcher; 10 years of experience) who confirmed the latency annotations. We note that the aforementioned experts are co-authors of this study. However, the dataset was collected and the latencies were annotated for two prior studies^{17,18} conducted before the conceptualization and development of DELMEP. Therefore, the annotations were performed independently of the development of the DELMEP algorithm. We performed an additional validation on an external MEP dataset annotated by three experts. From the three experts, one is a co-author of the present study. Data preprocessing and annotation was performed with custom-made scripts written in MATLAB R2017a (MathWorks Inc, USA). A total of 33,060 MEPs were recorded, i.e., 11,020 from each muscle group (abductor pollicis brevis, abductor digiti minimi, and first dorsal interosseous). From all MEPs, 232 (0.7%) were discarded because of pre-activation and 11,548 (34.9%) were discarded because of noise or no-response. Out of the remaining 21,244 MEPs, the

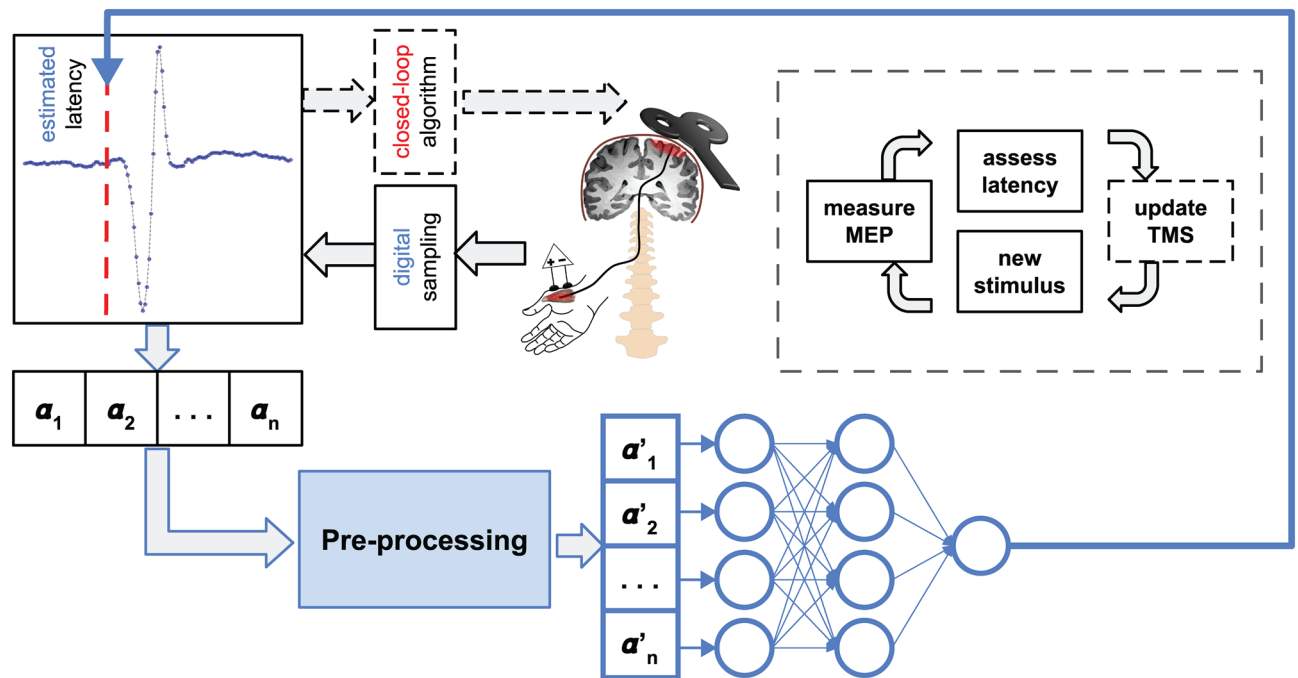


Figure 2. Workflow for automated assessment of MEP latencies in a possible closed-loop TMS set-up. MEPs are measured with electrodes placed on the target muscle and stored in a 120-dimension vector. The pre-processing is done by trimming, smoothing, centering, and normalizing the MEP. The resulting vector is used as an input to the neural network for the latency estimation. The dashed arrows show how our DELMEP algorithm could be applied to a closed-loop protocol (dashed box), in which the brain stimulation parameters are modified depending on the MEP responses.

validator discarded 4569 (21.5%) and approved 16,675 (78.5%). Therefore, in total, the dataset is composed of 16,675 MEPs and their peak-to-peak amplitudes and latencies.

Latency estimation algorithm. To automate the MEP latency assessment, we developed an algorithm named DELMEP, written in Python 3.8 and available at <https://github.com/connect2brain/delmepe>. The DELMEP pipeline is composed of the following steps (Fig. 2): (1) pre-processing and (2) latency estimation with a neural network. We present the details of each step below.

Pre-processing (step 1): The pre-processing simplifies the training and use of our neural network. Without the pre-processing, the high variability and noise of the MEPs would require that the neural network “learns” different inputs (MEP traces) corresponding to similar outputs (latencies). Here, the MEPs are represented by a mathematical vector of the raw voltage measurements, significantly reducing the complexity and increasing the speed of deep learning algorithms necessary to process the data. Hence, in this step, the data are (1) trimmed, (2) smoothed, (3) centered, and (4) amplitude normalized. The MEPs are trimmed from 10 to 50 ms after the TMS (120 samples). This is done to reduce and standardize their length, because in the resting condition, the measurements shortly after the TMS and much later than the end of the MEP do not carry relevant information. On the contrary, their inherent noise could pose a problem to the training and use of the neural network, since it would unnecessarily increase the dimensions of the input vectors.

After trimming, the MEPs are smoothed with a moving average filter with a window length of 3 samples, to reduce the high-frequency noise of the recordings²⁰. Next, the MEPs are centered by computing their mean value in the first 15 samples (5 ms) and then subtracting it from every sample. This step reduces the impact of low-frequency noise in the measurements, by counteracting the shifting it produces in the mean MEP value. The window length in the smoothing step and the time window in the centering step were tuned employing a grid search algorithm. Lastly, we normalize the MEPs so that their minimum and maximum values correspond to 0 and 1, respectively, to mitigate the effects of the large variations in amplitude. A detailed representation of this preprocessing is illustrated in Fig. 3, where the changes on the two MEPs presented in Fig. 1 are shown.

Deep learning algorithm (step 2): The pre-processed MEPs are used as inputs to the neural network, which produces a latency prediction as its output. This neural network is built as a multi-layer fully connected perceptron layout with two hidden layers of 30 artificial neurons each, and an output layer. We used the rectified linear unit activation function and trained the network with the Adam optimizer²¹ (early stopping criteria: 200 epochs; batch size: 32), as implemented in the software package Keras 2.4.3²².

Data analysis and method validation. From all MEPs, 2113 (13%) are low amplitude (peak-to-peak amplitude (V_{pp}) ≤ 100 μ V), 2995 (18%) are medium amplitude (100 μ V $< V_{pp} \leq 200$ μ V) and 11,565 (69%) are high amplitude ($V_{pp} > 200$ μ V). The MEPs were first divided randomly into a training (13,340 MEPs) and test-

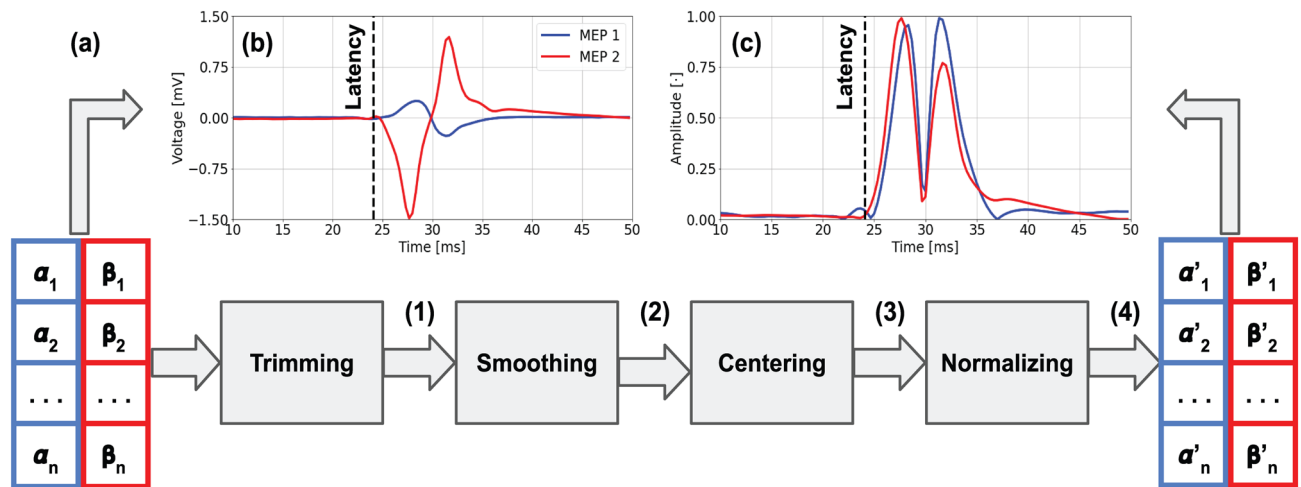


Figure 3. (a) Pre-processing of the two MEPs shown in Fig. 1, divided into: trimming (1), smoothing (2), centering (3) and normalizing (4). Panels (b) and (c) show the MEPs before and after the pre-processing, respectively. When comparing (b) and (c), note that the different MEPs look similar after the pre-processing, thus facilitating the training and later use of the neural network.

ing (3335 MEPs) dataset, with a training/testing ratio of 80/20. We verified the accuracy and repeatability of our method by using it to evaluate the latency of the 13,340 and 3335 MEPs in the training and testing datasets, respectively, and comparing these results with the manual assessment of the expert. The comparison was made by computing the mean absolute error (MAE) between the latencies provided by our method and those provided by the expert. We analyzed the latency prediction error by computing the correlation of the automated latency estimate with the two main MEP features: V_{pp} and the manually annotated latency. We also estimated the computational times for the DELMEP algorithm using a standard desktop computer (CPU Intel Core i7-5650U 2.2 GHz and 8 GB of RAM).

For comparison, we used the following algorithms: Signal Hunter⁹, AHTE¹⁰, SHTE¹⁰ and Bigoni's method¹¹ to estimate the latency of the MEPs in the testing dataset. These estimations were then compared to the manual annotations of the expert and the MAE was computed for every method. Signal Hunter is an open source software for MEP analysis having a latency estimation algorithm based on statistical measures, it performs a moving average filtering on the MEP, differentiates the smoothed signal, calculates the standard deviation (SD), and finds the index value for which the difference between the absolute differentiated MEP value and the SD is the largest; thereafter, it estimates the MEP latency by subtracting a user-selected *magic number* from that index value. We implemented Signal Hunter with a magic number equal to 5, following the author's original implementation⁹. The AHTE algorithm performs an absolute value operation on the MEP, finds its maximum amplitude and determines the threshold value (V_{thr}), marks $\pm 10\%$ around the mean value of the MEP, and finds the index value where the marked line is crossed by the MEP for the first time. The latency estimation is obtained by subtracting a user-selected magic number from that index value. The SHTE algorithm is based on the same principle as the AHTE algorithm, but it works by squaring the MEP coefficients, instead of performing an absolute value operation. We implemented the AHTE and SHTE algorithms ($V_{thr} = 10\%$ and magic number = 5) as done in¹⁰. Bigoni's method is a derivative-based method, it reduces the MEP to a window of 10–50 ms after the stimulation, finds the peak and trough of the MEP, performs an absolute value operation, computes the approximate first derivative of the MEP until the peak, finds the longest vector of consecutive samples having a positive derivative, and estimates the latency as the first sample of this vector. All algorithms were implemented in Python 3.8.

To evaluate the generalizability of our DELMEP algorithm, we performed a cross-validation both within and across subjects. In a within-subject test, the data of each subject was split in 5 folds; 80% of the MEPs were used as training dataset and the remaining 20% as the validation set, interchangeably. Final results were obtained by computing the average MAE and SD of MAE across folds for each subject separately. The inter-subject variability of our DELMEP algorithm was tested using a leave-one-subject-out approach. In this test, the data from all but one subject was used to train the model and the MAE was estimated using the data from the left-out subject. This was repeated for all subjects and the MAE was computed in every iteration.

An additional validation was performed in which our DELMEP algorithm and Bigoni's method were used to estimate the latency of the MEPs in an independent dataset, which is composed of 1561 MEPs and described in detail in the study by Bigoni et al.¹¹. This dataset was collected from 16 healthy volunteers (eight women and eight men; age: 26.7 ± 2.6 years). The latencies were manually annotated by three different experts (with 0.5, 5 and 14 years of experience) who did not take part in the development of DELMEP. For validating DELMEP, we computed the ground truth (GT) latency as the mean value from the three annotations. About 99% of the MEPs in this dataset have a high amplitude ($V_{pp} > 100 \mu V$), as these MEPs were collected using a single-pulse paradigm, with a test-intensity chosen to produce MEP amplitude of 0.50 mV.

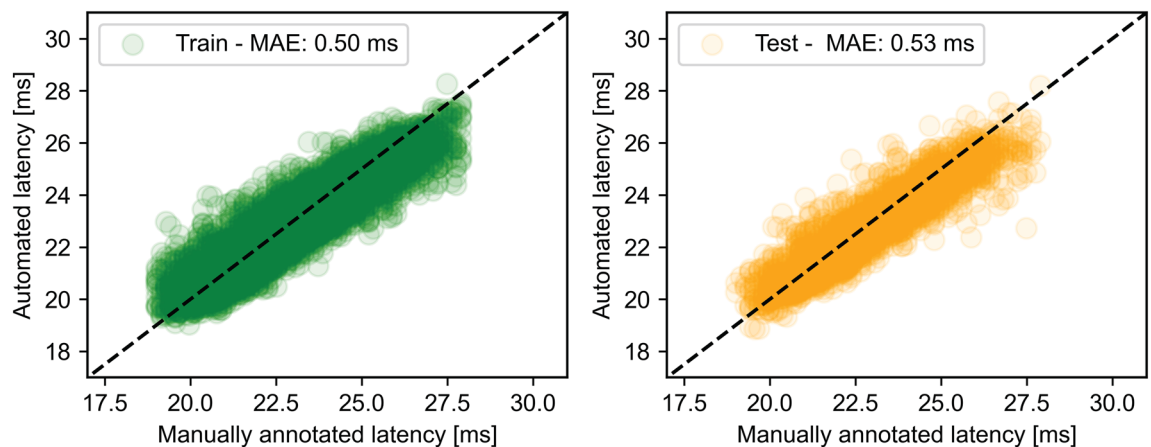


Figure 4. Automated MEP latency annotations with the proposed DELMEP algorithm in the training dataset (green) and testing dataset (orange). The results are compared to the manually assessed values. The MAE is presented for both datasets.

Results

Training the neural network on a dataset of 13,340 MEPs required about 2 min and pre-processing an MEP trace required 1.2 ms. On average, annotating a pre-processed MEP required 65 μ s. The estimated MEP latencies by the DELMEP algorithm and corresponding MAE, for the testing and training datasets are illustrated in Fig. 4. The similarity between the automated DELMEP and the manual expert annotation suggests a successful training process, since the MEPs in the testing dataset were not used to train the neural network.

To provide a practical example of the DELMEP performance, Fig. 5 shows eight MEPs and their corresponding automated and manually annotated latencies. Although such a small sample can only be considered as an illustrative example, it provides a notion of how the proposed algorithm performs when used to replace a human expert in MEP annotations.

Figure 6 illustrates the error associated with the DELMEP algorithm for the corresponding MEP V_{pp} and manually annotated latency. The sub-panel shows the correlation between the DELMEP latency estimation error and the MEP V_{pp} for MEPs with an estimation error equal or higher than 1 ms. From the 3,335 MEPs assessed by DELMEP in the testing dataset, 1,895 (57%) had an error lower than 0.5 ms and 2924 (88%) had an error lower than 1 ms, making it useful not just in research but also in clinical medical practice.

The results from the validation comparison between DELMEP and Signal Hunter, AHTE, SHTE, and Bigoni's method can be found in Table 1, where the MAE is reported for the entire testing dataset and also divided between high- and low-amplitude MEPs. It is important to notice that Bigoni's method discards MEPs when it is not able to find a long enough vector of samples with positive derivatives. The minimum number of samples with positive derivatives in our implementation was set to five, following the original author's implementation¹¹. This resulted in 483 out of 3335 MEPs in the testing dataset (15%), most of which corresponded to low-amplitude MEPs, being discarded by Bigoni's method. To make a direct comparison, only the remaining MEPs were considered to compute the MAE of every method. However, we note that for the cross-validation, in Table 2, the entire dataset was used.

The resulting MAE from the five-fold cross-validation when using each batch for testing is reported in Table 2, together with the average MAE for all tests and its SD.

The intra-subject variability was analyzed by computing a five-fold cross-validation using data from one subject at a time, and repeating the process for all subjects. The MAE for each data batch of each subject is reported in Table 3, together with the average and SD for all tests. Furthermore, the correlation between error and dataset size for every subject is shown in Fig. 7, together with a fitted curve.

The inter-subject variability was analyzed by using the data of one of the subjects for testing and the data from the remaining eight subjects for training; this process was repeated for each subject. The MAE for each subject together with the average and SD for all tests are reported in Table 4.

Figure 8 shows the results for the additional validation using the dataset from Bigoni et al.¹¹. The MAE from DELMEP was 0.7 ms, while that of Bigoni's method was 0.4 ms. In the case of DELMEP, the highest errors correspond to high-latency MEPs (above 28 ms).

Discussion

Our DELMEP algorithm performed better than traditional hard-threshold based algorithms across different MEP amplitude ranges. This improved performance is especially valuable for low-amplitude MEPs, commonly recorded at low stimulation intensities, when computing the motor threshold and in inhibitory paired-pulse paradigms^{18,23,24}. For example, with the same low-amplitude MEPs ($V_{pp} \leq 100$ μ V) in the testing dataset, DELMEP, Bigoni's method, SHTE, AHTE and Signal Hunter yielded an MAE of 0.6, 1.0, 7.3, 16.5 and 22.9 ms, respectively; with DELMEP being about one order of magnitude more accurate than these algorithms. On the other hand, with the same high-amplitude MEPs ($V_{pp} > 100$ μ V) in the testing dataset, DELMEP, Bigoni's method, SHTE, AHTE and Signal Hunter yielded an MAE of 0.5, 0.8, 1.3, 2.8 and 6.3 ms, respectively. This is possibly due to the

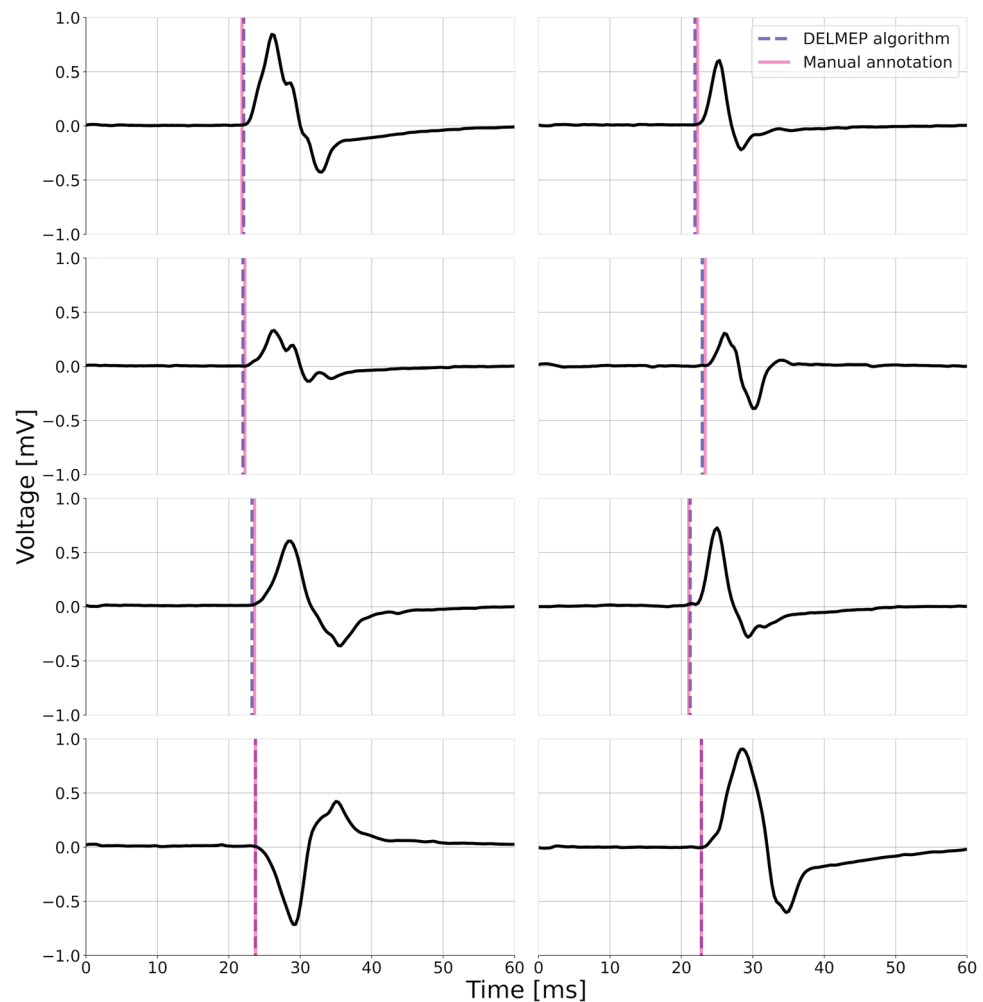


Figure 5. Illustrative MEPs from the testing dataset and their corresponding automated (dashed violet vertical line) and manually assessed (purple vertical line) latencies. These MEPs were not used to train the neural network. The similarity between both latencies indicates the successful performance of our DELMEP algorithm.

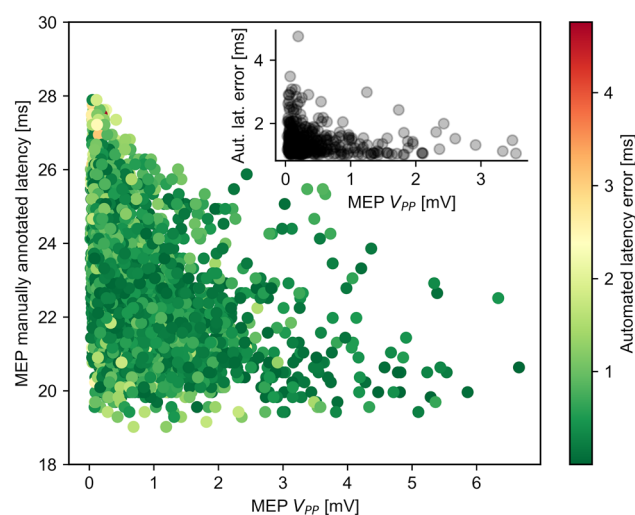


Figure 6. Map of the DELMEP algorithm errors in estimating MEP latencies, as a function of the MEP V_{pp} amplitude and manually annotated latency. The upper-right panel shows the DELMEP estimation error versus the MEP V_{pp} amplitude, for MEPs with latency estimation error higher than 1 ms.

Method	MAE—low amplitude MEPs ($V_{pp} \leq 100 \mu V$) [ms]	MAE—high amplitude MEPs ($V_{pp} > 100 \mu V$) [ms]	MAE—all MEPs [ms]
Signal hunter	22.9	6.3	7.7
AHTE	16.5	2.8	4.0
SHTE	7.3	1.3	1.8
Bigoni's method	1.0	0.8	0.8
DELMEP	0.6	0.5	0.5

Table 1. Comparison of mean absolute errors (MAE) obtained with DELMEP, Signal Hunter, AHTE, SHTE, and Bigoni's method for the MEPs in the testing dataset. The MAE is reported for the entire dataset and for low/high amplitude MEPs. MEPs discarded by Bigoni's method were also discarded on the other methods for a direct comparison.

Cross-validation MAE [ms]					Average MAE [ms]	SD [ms]
1	2	3	4	5		
0.5	0.5	0.5	0.5	0.6	0.5	0.03

Table 2. Cross-validation of DELMEP across the entire dataset. The available data was divided into five different batches. In each test, one of the batches was used to test the algorithm and the remaining batches to train it. The mean absolute error (MAE) is reported for every batch, as well as its average and standard deviation (SD) for all batches.

Subject N°	Cross-validation mean absolute error (MAE) [ms]					Average MAE [ms]	SD [ms]
	1	2	3	4	5		
1	0.6	0.7	0.6	0.8	0.6	0.7	0.08
2	0.5	0.5	0.5	0.5	0.5	0.5	0.01
3	0.6	0.6	0.6	0.6	0.6	0.6	0.02
4	0.7	0.7	1.0	0.9	1.0	0.9	0.14
5	0.5	0.6	0.6	0.6	0.5	0.5	0.03
6	0.5	0.6	0.5	0.6	0.6	0.6	0.03
7	0.5	0.5	0.5	0.5	0.6	0.5	0.03
8	0.6	0.6	0.6	0.6	0.7	0.6	0.05
9	0.4	0.5	0.5	0.4	0.5	0.5	0.04

Table 3. Intra-subject variability of DELMEP. A five-fold cross-validation was performed using data from one subject at a time, the process was repeated for all subjects. The table contains the mean absolute error (MAE) for every data batch of each subject, together with the average and standard deviation (SD) for every subject.

consistent accuracy of our DELMEP algorithm regardless of the MEP amplitude. Such higher prediction errors correlated with lower MEP amplitudes can be explained by the inherently lower SNR, which has a stronger effect on methods relying on hard-threshold estimators¹⁰.

When tested in our larger dataset (Table 1), the automated annotation by DELMEP was on average 0.3 ms more accurate than the state-of-the-art derivative-based Bigoni's method. Both DELMEP and Bigoni's method retain their accuracy on low-amplitude MEPs, an important feature which is out of reach for all previously tested algorithms. When applied to Bigoni's dataset (Fig. 8), DELMEP shows a slightly larger error than Bigoni's method (0.7 ms and 0.4 ms, respectively). We should note that Bigoni's method discarded 61 out of the 1561 MEPs in the dataset (approximately 4%), of which it was not able to estimate the corresponding latencies. Interestingly, the highest MAE of DELMEP corresponded to MEPs with latencies above 28 ms. This can probably be explained by the fact that the MEP dataset used to train DELMEP had latencies mostly below 28 ms (see Fig. 4), which could potentially affect the performance of the method. Nevertheless, DELMEP and Bigoni's method show a similar accuracy for general applications and are about an order of magnitude more accurate than traditional hard-threshold algorithms.

From the user point of view, both DELMEP and Bigoni's algorithms work by providing the MEP trace as an input and obtaining the estimated latency as an output. The machine learning nature of DELMEP makes it a more complex algorithm than Bigoni's method. However, this does not translate into a disadvantage for the user, since the code made available with this publication is ready-to-use and no experience in machine learning

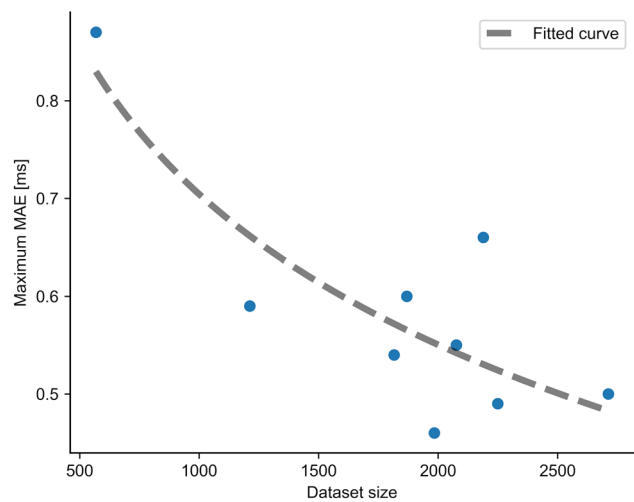


Figure 7. Relation between the average MAE obtained during the intra-subject cross-validation tests and the dataset size of every subject (number of MEPs). Each data point represents a different subject in the dataset.

Inter-subject mean absolute error (MAE) [ms]									Average MAE [ms]	SD [ms]
1	2	3	4	5	6	7	8	9		
0.7	0.6	0.7	0.5	0.6	0.6	0.5	0.7	0.5	0.6	0.1

Table 4. Inter-subject variability of DELMEP. The data from one subject was used for testing and the data from the remaining subjects for training. This process was repeated for every subject. The mean absolute error (MAE) for every subject, together with its average and standard deviation (SD) are reported.

is required for using it in research and/or clinical applications. Re-training DELMEP on a new training dataset requires just minor changes to the source code and a few seconds of running time in a regular desktop computer. Both algorithms require minimal human labor time and, unless modifications to the code are intended, minimal interventions and technical knowledge as well.

From a technical point of view, the main difference between DELMEP and Bigoni’s method is that the former is a machine learning algorithm, which “learns” how to annotate MEPs through a dataset of examples; while the latter is a rule-based algorithm, which finds the latency of MEPs by following a static set of steps. This makes Bigoni’s method simpler and a more explicable algorithm than DELMEP. However, an important advantage of our deep learning approach is the possibility to pre-train and apply the neural networks on application-specific datasets. For instance, separate models can be created for MEPs from the leg, forearm, and hand muscles, which naturally have distinct latencies^{25,26}. Therefore, this approach may provide more accurate automated annotations for a wider set of applications. Deep learning algorithms can also be used in active-learning processes to constantly and automatically improve the accuracy of their annotations^{27–29}, by periodically retraining them on data generated during their utilization. This is of special importance for applications on personalized medicine. As depicted in Fig. 7, when training and testing on data from a single subject, the latency estimation errors were noticeably reduced as the size of the available dataset was increased. Thus, the proposed DELMEP algorithm could be trained on already-available annotated MEPs of one particular subject, and thereafter used to automate the annotation of MEPs of this subject, in order to ensure the best possible accuracy. This is a feature that non-machine learning algorithms do not have, due to their static set of rules.

We should note that a deep learning-based algorithm requires a large dataset for training. However, for a research lab already performing experiments using MEPs, there might be a suitable dataset available, since just a few sessions can produce thousands of MEPs. Data from previous studies are useful even if they were recorded on different muscles and using a different setup (e.g., with a different sampling frequency or stimulation paradigm). Moreover, if more MEPs are required, there is no need for the same expert to annotate them. However, DELMEP would benefit from different experts annotating different sections of the dataset, as that would reduce the chance of the algorithm overfitting to biases that could be present in a single expert (e.g., a tendency to under- or over-estimate MEPs latencies). In this regard, we note that DELMEP was trained on MEPs annotated by a single expert. There was a 0.20 ms increase in the MAE (0.50–0.70 ms) when comparing the results from testing against the same expert used for the training, and a committee of three independent experts on a different dataset. This increase could be partially caused by having used a single expert to annotate the MEPs in the training dataset. However, this is still a state-of-the art accuracy. Moreover, using a single expert to annotate the latencies facilitates and drastically speeds up the process. On the other hand, the MAE of Bigoni’s method

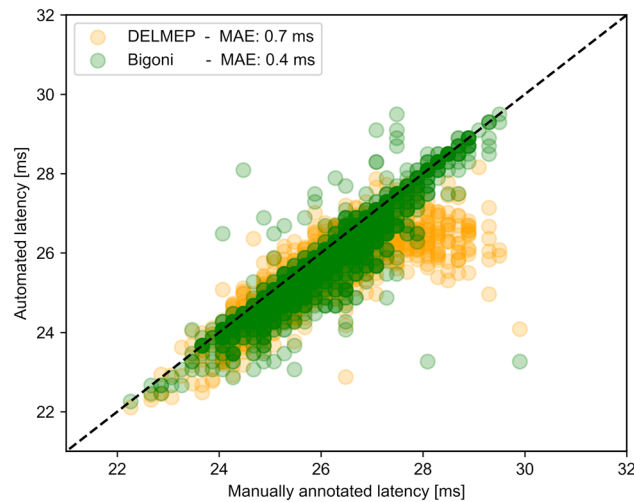


Figure 8. Latencies annotated with DELMEP and Bignoni's method vs manually annotated latencies for the MEPs in Bigoni's dataset. The manually annotated latencies are the mean value of the annotations of three independent experts.

when tested on their own dataset versus on our dataset increased 0.40 ms (from 0.40 to 0.80 ms), indicating that a variation in accuracy of this magnitude is possible even if the algorithm is not based on machine learning. As a reference, Bigoni et al.¹¹ found a difference of about 0.40 ms when comparing the estimation of two experts.

We should also emphasize that the low computational cost associated with our DELMEP algorithm allows it to be efficiently used in real-time closed-loop brain stimulation protocols^{30,31} and combined with multi-coil TMS electronic targeting for fast and automated cortical mappings^{32–34}, as it requires roughly 1 ms to process an MEP in a regular desktop computer.

Conclusions

We developed a deep learning-based algorithm to annotate MEP latencies automatically without the need for a human expert intervention. The main difference between our algorithm and previously reported solutions is that the deep learning nature of DELMEP allows it to learn and improve based on the available data, making it an ideal candidate for personalized clinical applications. The accuracy of our DELMEP algorithm was practically independent of the amplitude of the MEP, a feature only found in Bigoni's method, as all threshold-based algorithms considered in this study failed this test. We demonstrated that DELMEP has a high accuracy on two independent datasets. The millisecond-level automated annotation in our proposed DELMEP algorithm opens a possibility for real-time assessment of MEP latencies in closed-loop brain stimulation protocols.

Data availability

The data will be provided upon a reasonable request (including but not limited to reproducibility and further related analysis). Requests should be sent to the corresponding author and the data confidentiality requirements should be strictly followed according to our ethical permission statement. The Python implementation of the DELMEP algorithm used in this study is available at <https://doi.org/10.5281/zenodo.7920467> and the repository for development can be accessed at <https://github.com/connect2brain/delmep>.

Received: 29 August 2022; Accepted: 8 May 2023

Published online: 22 May 2023

References

- Emerson, R. G. Evoked potentials in clinical trials for multiple sclerosis. *J. Clin. Neurophysiol.* **15**, 109–116 (1998).
- Macdonell, R. A., Donnan, G. A. & Bladin, P. F. A comparison of somatosensory evoked and motor evoked potentials in stroke. *Ann. Neurol.* **25**, 68–73 (1989).
- Chowdhury, F. A. et al. Motor evoked potential polyphasia: A novel endophenotype of idiopathic generalized epilepsy. *Neurology* **84**, 1301–1307 (2015).
- Brown, K. E. et al. The reliability of commonly used electrophysiology measures. *Brain Stimul.* **10**, 1102–1111 (2017).
- Livingston, S. C. & Ingersoll, C. D. Intra-rater reliability of a transcranial magnetic stimulation technique to obtain motor evoked potentials. *Int. J. Neurosci.* **118**, 239–256 (2008).
- Krieg, S. M. et al. Protocol for motor and language mapping by navigated TMS in patients and healthy volunteers; workshop report. *Acta Neurochir.* **159**, 1187–1195 (2017).
- Giridharan, S. R. et al. Motometrics: A toolbox for annotation and efficient analysis of motor evoked potentials. *Front. Neuroinform.* **13**, 8. <https://doi.org/10.3389/fninf.2019.00008> (2019).
- Harquel, S. et al. Cortextool: A toolbox for processing motor cortical excitability measurements by transcranial magnetic stimulation. <https://hal.archives-ouvertes.fr/hal-01390016> (2016).
- Souza, V. H., Peres, A., Zacharias, L. & Baffa, O. SignalHunter: Software for electrophysiological data analysis and visualization. <https://doi.org/10.5281/zenodo.1326308> (2018).

10. Šoda, J., Vidaković, M. R., Lorincz, J., Jerković, A. & Vujović, I. A novel latency estimation algorithm of motor evoked potential signals. *IEEE Access* **8**, 193356–193374 (2020).
11. Bigoni, C., Cadic-Melchior, A., Vassiliadis, P., Morishita, T. & Hummel, F. C. An automatized method to determine latencies of motor-evoked potentials under physiological and pathophysiological conditions. *J. Neural Eng.* **19**, 024002 (2022).
12. Sollmann, N. *et al.* The variability of motor evoked potential latencies in neurosurgical motor mapping by preoperative navigated transcranial magnetic stimulation. *BMC Neurosci.* **18**, 1. <https://doi.org/10.1186/s12868-016-0321-4> (2017).
13. Kiers, L., Cros, D., Chiappa, K. H. & Fang, J. Variability of motor potentials evoked by transcranial magnetic stimulation. *Electroencephalogr. Clin. Neurophysiol.* **89**, 415–423 (1993).
14. Wassermann, E. M. Variation in the response to transcranial magnetic brain stimulation in the general population. *Clin. Neurophysiol.* **113**, 1165–1171 (2002).
15. Picht, T. *et al.* Assessing the functional status of the motor system in brain tumor patients using transcranial magnetic stimulation. *Acta Neurochir.* **154**, 2075–2081 (2012).
16. Schmidhuber, J. Deep learning in neural networks: An overview. <https://arxiv.org/abs/1404.7828> (2014).
17. Souza, V. H. *et al.* TMS with fast and accurate electronic control: Measuring the orientation sensitivity of corticomotor pathways. *Brain Stimul.* **15**, 306–315 (2022).
18. Souza, V. H. *et al.* Probing the orientation specificity of excitatory and inhibitory circuitries in the primary motor cortex with multi-channel TMS. *bioRxiv* **2021**, 56 (2021).
19. Koponen, L. M., Nieminen, J. O. & Ilmoniemi, R. J. Multi-locus transcranial magnetic stimulation—theory and implementation. *Brain Stimul.* **11**, 849–855 (2018).
20. Makridakis, S. G., Wheelwright, S. C. & Hyndman, R. J. *Forecasting: Methods and Applications* (Wiley, 1998).
21. Diederik, P. & Lei Ba, J. Adam: A method for stochastic optimization. <https://arxiv.org/abs/1412.6980> (2015).
22. Chollet, F. *et al.* Keras. <https://github.com/fchollet/keras> (2015).
23. Ziemann, U., Rothwell, J. C. & Ridding, M. C. Interaction between intracortical inhibition and facilitation in human motor cortex. *J. Physiol.* **496**, 873–881 (1996).
24. Ilić, T. V. *et al.* Short-interval paired-pulse inhibition and facilitation of human motor cortex: The dimension of stimulus intensity. *J. Physiol.* **545**, 153–167 (2022).
25. Wassermann, E. M. *et al.* *The Oxford Handbook of Transcranial Stimulation* (Oxford University Press, 2021).
26. Rossini, P. M. *et al.* Non-invasive electrical and magnetic stimulation of the brain, spinal cord, roots and peripheral nerves: Basic principles and procedures for routine clinical and research application. An updated report from an I.F.C.N. Committee. *Clin. Neurophysiol.* **126**, 1071–1107 (2015).
27. Ren, P. *et al.* A survey of deep active learning. <https://arxiv.org/abs/2009.00236> (2020).
28. Shen, Y. *et al.* Deep active learning for named entity recognition. <https://arxiv.org/abs/1707.05928> (2017).
29. Zhang, L., Lin, D., Wang, H. & Car, R. E. W. Active learning of uniformly accurate interatomic potentials for materials simulation. *Phys. Rev. Mater.* **3**, 023804 (2019).
30. Zrenner, B. *et al.* Brain oscillation-synchronized stimulation of the left dorsolateral prefrontal cortex in depression using real-time EEG-triggered TMS. *Brain Stimul.* **13**, 197–205 (2020).
31. Zrenner, C., Desideri, D., Belardinelli, P. & Ziemann, U. Real-time EEG-defined excitability states determine efficacy of TMS-induced plasticity in human motor cortex. *Brain Stimul.* **11**, 374–389 (2008).
32. Tervo, E. A. *et al.* Automated search of stimulation targets with closed-loop transcranial magnetic stimulation. *Neuroimage* **220**, 117082 (2020).
33. Tervo, E. A. *et al.* Closed-loop optimization of transcranial magnetic stimulation with electroencephalography feedback. *Brain Stimul.* **15**, 523–531 (2022).
34. Nieminen, J. O. *et al.* Multi-locus transcranial magnetic stimulation system for electronically targeted brain stimulation. *Brain Stimul.* **15**, 116–124 (2022).

Acknowledgements

We acknowledge the computational resources provided by the Aalto Science-IT project.

Author contributions

D.M.: conceptualization, methodology, investigation, formal analysis, software, resources, visualization, writing—original draft, writing—review & editing. V.H.S.: conceptualization, methodology, investigation, formal analysis, software, resources, visualization, writing—original draft, writing—review & editing. I.Z.: conceptualization, resources, software, methodology, writing—review & editing. S.T.: data collection, resources, writing—review & editing. J.O.N.: resources, writing—review & editing. C.B.: data collection, resources, writing—review & editing. F.C.H.: data collection, resources, writing—review & editing. J.T.K.: resources, conceptualization, methodology, writing—review & editing. D.A.: writing—review & editing. P.L.: data collection, resources, writing—review & editing. N.T.: methodology, formal analysis, software, writing—review & editing. T.G.: writing—review & editing. R.J.I.: conceptualization, writing—review & editing.

Funding

This research has received funding from the Academy of Finland (Decision Nos. 255347, 265680, 294625, 306845, 348631, and 349985), the Finnish Cultural Foundation, Jane and Aatos Erkko Foundation, Erasmus Mundus SMART2 (No. 552042-EM-1-2014-1-FR-ERA MUNDUSEMA2), the Conselho Nacional de Desenvolvimento Científico e Tecnológico (CNPq; grant number 140787/2014-3), the European Research Council (ERC) under the European Union's Horizon 2020 research and innovation programme (ConnectToBrain, grant agreement No. 810377), Personalized Health and Related Technologies (PHRT #2017-205) of the ETH Domain, Defitech Foundation and the Wyss Center for Bio and Neuroengineering.

Competing interests

R.J.I. has been an advisor and is a minority shareholder of Nexstim Plc. J.O.N. and R.J.I. are inventors on patents and patent applications on TMS technology. P.L. has received consulting fees (unrelated to this work) from Nexstim Plc. The other authors declare no conflict of interest.

Additional information

Correspondence and requests for materials should be addressed to D.M.

Reprints and permissions information is available at www.nature.com/reprints.

Publisher's note Springer Nature remains neutral with regard to jurisdictional claims in published maps and institutional affiliations.



Open Access This article is licensed under a Creative Commons Attribution 4.0 International License, which permits use, sharing, adaptation, distribution and reproduction in any medium or format, as long as you give appropriate credit to the original author(s) and the source, provide a link to the Creative Commons licence, and indicate if changes were made. The images or other third party material in this article are included in the article's Creative Commons licence, unless indicated otherwise in a credit line to the material. If material is not included in the article's Creative Commons licence and your intended use is not permitted by statutory regulation or exceeds the permitted use, you will need to obtain permission directly from the copyright holder. To view a copy of this licence, visit <http://creativecommons.org/licenses/by/4.0/>.

© The Author(s) 2023